A Fully Automatic Unsupervised Segmentation Framework for the Brain Tissues in MR images

Qaiser Mahmood [*a, b], Artur Chodorowski [a, b], Babak Ehteshami Bejnordi [c], Mikael Persson [a, b]
[a]Department of Signals and Systems, Chalmers University of Technology, Gothenburg, Sweden,
[b]MedTech West, Sahlgrenska University Hospital, Gothenburg, Sweden, [c] Dept. of Radiology,
Radboud University Medical Center, Nijmegen, The Netherlands

ABSTRACT

This paper presents a novel fully automatic unsupervised framework for the segmentation of brain tissues in magnetic resonance (MR) images. The framework is a combination of our proposed Bayesian-based adaptive mean shift (BAMS), *a* priori spatial tissue probability maps and fuzzy c-means. BAMS is applied to cluster the tissues in the joint spatial-intensity feature space and then a fuzzy c-means algorithm is employed with initialization by *a* priori spatial tissue probability maps to assign the clusters into three tissue types; white matter (WM), gray matter (GM) and cerebrospinal fluid (CSF). The proposed framework is validated on multimodal synthetic as well as on real T1-weighted MR data with varying noise characteristics and spatial intensity inhomogeneity. The performance of the proposed framework is evaluated relative to our previous method BAMS and other existing adaptive mean shift framework. Both of these are based on the mode pruning and voxel weighted k-means algorithm for classifying the clusters into WM, GM and CSF tissue. The experimental results demonstrate the robustness of the proposed framework to noise and spatial intensity inhomogeneity, and that it exhibits a higher degree of segmentation accuracy in segmenting both synthetic and real MR data compared to competing methods.

Keywords: Magnetic resonance, brain segmentation, spatial tissue probability map, mean shift, fuzzy c-means

1. INTRODUCTION

Accurate segmentation in Magnetic resonance (MR) images plays a vital role for the quantitative analysis of normal and abnormal brain tissues [1-3]. It can also be useful for assigning individual tissues conductivity to constructing the realistic conductivity models for various neurological applications such as electroencephalography (EEG) source localization in epilepsy patients [4,5] and hyperthermia treatment planning for head and neck [6,7]. Accurate segmentation of tissues in MR brain images is a challenging task because of noise and spatial intensity inhomogeneity artifacts [8-11]. Several unsupervised segmentation methods [12-16] have been proposed to cope with these problems. However, the main disadvantage of these methods is that they rely on many critical parameter settings to segment the tissues accurately in MR brain images [17].

Mean shift (MS) [18,19] is one of the unsupervised clustering methods, which doesn't have this problem. It is an adaptive gradient approach to estimate the modes of the multivariate distribution underlying the feature space. The feature points that are associated with a mode form a cluster. The only parameter that influences the clustering is the bandwidth of the kernel. However, the use of a fixed bandwidth can cause over-clustering or under-clustering. Several approaches [20-22] have been proposed to solve this problem, wherein the bandwidth of each feature point is used to estimate the clusters. Therefore, the mean shift based on the adaptive bandwidth of the kernel is called adaptive mean shift (AMS).

* qaiserm@chalmers.se, Tel: +46 73-6672173; Fax: +46 31-7721725

Medical Imaging 2014: Biomedical Applications in Molecular, Structural, and Functional Imaging,
edited by Robert C. Molthen, John B. Weaver, Proc. of SPIE Vol. 9038, 90381M
© 2014 SPIE · CCC code: 1605-7422/14/$18 · doi: 10.1117/12.2043646

Downloaded From: http://spiedigitallibrary.org/ on 09/29/2014 Terms of Use: http://spiedl.org/terms

AMS can also provide clustering by taking both the spatial and the intensity domain into account. Due to this characteristic, AMS can be more robust to noise and spatial intensity inhomogeneity artifacts in the MR brain images compared to intensity based clustering methods [17]. The output of the AMS is a set of clusters or modes. In order to get the desired number of clusters or tissue classes, merging is required.

In [17], the first adaptive mean shift framework is proposed for segmenting the brain tissues in the MR images. The framework is based on the mode merging and voxel weighted k-means algorithm to categorize the clusters, obtained from the adaptive mean shift, into WM, GM and CSF tissue. In our previous work [22], we proposed a Bayesian based adaptive mean shift (BAMS) method wherein we adopt the same procedure as described in [17] for assigning the clusters into three tissue types.

A downside of this procedure is that mode pruning in a range (intensity) domain can lose spatial information of modes (clusters), which may cause combining of the modes belonging to different tissue classes. Another downside of it is that the final merging of pruned modes into three tissue types, using the prior knowledge about the ordering of tissue intensity [17] in MR images to initialize the voxel weighted k-means algorithm, may also lead to assigning the clusters to the wrong tissue class.

To overcome this problem, we here propose a new unsupervised segmentation framework, wherein we incorporate the spatial priors of the tissues to assigning the clusters, obtained from the adaptive mean shift, into the three tissue types; WM, GM and CSF. The proposed framework is based on the Bayesian-based adaptive mean shift (BAMS), *a* priori spatial tissue probability maps and the fuzzy c-means algorithm.

The organization of the paper is as follows. Section 2 describes the MR data and the proposed framework. The experimental results for both synthetic and real MR data are presented in section 3. Section 4 discusses the results and finally, the conclusions are drawn in section 5.

2. Materials and Methods

2.1. MRI data

We used two different data sets to evaluate the performance of our proposed framework relative to our previous method [22] as well as other competing adaptive mean shift (AMS) framework [17]. These data sets are hereinafter referred to as data set 1 and data set 2.

Data set 1 comprises synthetic multimodal MR data, obtained from the BrainWeb simulated brain database (SBD) [23]. More specifically the data set comprises realistic T1, T2, and proton density (PD) MR images for four different noise levels (3%, 5%, 7% and 9%) with two different spatial intensity inhomogeneity levels (20% and 40%). Each MR image is of size 181×217×181 with cubic voxels of size $1\ mm^3$.

Data set 2 comprises five real T1 MR images of healthy subjects, downloaded from the IBSR [24] database. Each MR image consists of 60 coronal T1 slices. The size of each voxel is $3.1\ mm^3$.

A ground truth segmentation for each data set was also obtained from their corresponding databases.

2.2. Bayesian-based adaptive mean shift (BAMS)

In [22], we proposed an adaptive bandwidth estimator based on the Bayesian approach for the estimation of bandwidth of the kernel. The approach includes the modelling of local variances of N set of neighborhoods of each feature point and fitting of Gamma distribution function to these. The estimated bandwidth for each feature point is then used in the mean shift to estimate the modes of multivariate distributions underlying the feature space. We called it Bayesian based adaptive mean shift (BAMS).

Downloaded From: http://spiedigitallibrary.org/ on 09/29/2014 Terms of Use: http://spiedl.org/terms

In BAMS, the mode or cluster of brain tissue is defined as

$$\mathbf{y}_{j+1} = \frac{\sum_{i=1}^{n} \frac{1}{h_i^{d+2}} \mathbf{x}_i \; g\left(\left\|\frac{\mathbf{y}_j - \mathbf{x}_i}{h_i}\right\|^2\right)}{\sum_{i=1}^{n} \frac{1}{h_i^{d+2}} g\left(\left\|\frac{\mathbf{y}_j - \mathbf{x}_i}{h_i}\right\|^2\right)} \qquad j = 1,2 \ldots \tag{1}$$

where $\{\mathbf{x}_i \in \mathbb{R}^d \mid i = 1, \ldots . n\}$ is a set of n feature vectors in d-dimensional space that represent a single or multimodal MR brain data, $g(x)$ is the kernel profile of kernel G, $h(\mathbf{x}_i) \equiv h_i$ is an adaptive bandwidth of the kernel for feature point $\mathbf{x}_i$ and $\{\mathbf{y}\}_{j=1,2\ldots}$ represents the successive locations of the kernel G.

The kernel G starts from an initial position $\mathbf{y}_1$ and moves towards the position closer to the higher dense region. This process is continued until the position in higher dense region is achieved which represents a mode (local maxima) of the density. The feature points that converge to the same mode constitute a cluster. In order to perform the clustering using spatial information of brain voxels with its intensity values, we used a joint spatial-intensity domain kernel G_{h_s,h_r}, defined as

$$G_{h_s,h_r}(\mathbf{x}) = \frac{c}{h_s^p h_r^d} g\left(\left\|\frac{\mathbf{x}^s}{h_s}\right\|^2\right) g\left(\left\|\frac{\mathbf{x}^r}{h_r}\right\|^2\right) \tag{2}$$

where $\mathbf{x}^s$ represents a vector of spatial coordinates of brain voxels, $\mathbf{x}^r$ represents a vector of brain voxels intensity values and h_s and $h_i \equiv h_r$ are their corresponding kernel bandwidths. In this work, we used Gaussian kernel for both spatial and intensity domain and set the spatial bandwidth to h_s = 3. The output of BAMS is a set of modes or clusters of brain tissues.

2.3. Fuzzy c-means algorithm

Let $\{\mathbf{z}_1, \mathbf{z}_2, \mathbf{z}_3, \ldots \ldots, \mathbf{z}_m\}$ denote a set of *m* clusters obtained from the BAMS. The fuzzy c-means [25] is then applied to assign these clusters to the three tissue types by minimizing the cost function defined as

$$J = \sum_{j=1}^{m} \sum_{k=1}^{c} p_{kj}^{g} \left\|\mathbf{I}_j - \mu_k\right\|^2 \qquad j = 1,2 \ldots . . m \tag{3}$$

where $\mathbf{I}_j$ represents an intensity vector of cluster $\mathbf{z}_j$, μ_k is the *k*th cluster (tissue) center and p_{kj} is known as membership function and it represents the probability that an intensity vector $\mathbf{I}_j$ of cluster $\mathbf{z}_j$ belongs to a specific tissue. The constant *g* controls the fuzziness of the resulting partition. In this work, we set *g* = 1.5.

To initialize the tissue centers, *a* priori spatial tissue probability maps are incorporated into the fuzzy c-means algorithm. The *k*th tissue center is then initialized as

$$\mu_{k\_initial} = \frac{\sum_{j=1}^{m} p_{kj\_initial}^{g} \mathbf{I}_j}{\sum_{j=1}^{m} p_{kj\_initial}^{g}} \tag{4}$$

where $p_{kj\_initial}$ represents *a* priori spatial probability map of *k*th tissue. The membership functions and tissue centers are then updated as

$$p_{kj} = \frac{1}{\sum_{i=1}^{c} \left(\frac{\left\|\mathbf{I}_j - \mu_k\right\|}{\left\|\mathbf{I}_j - \mu_i\right\|}\right)^{2/(g-1)}} \tag{5}$$

$$\mu_k = \frac{\sum_{j=1}^{m} p_{kj}^{g} \mathbf{I}_j}{\sum_{j=1}^{m} p_{kj}^{g}} \tag{6}$$

Downloaded From: http://spiedigitallibrary.org/ on 09/29/2014 Terms of Use: http://spiedl.org/terms

2.4. Summary of the proposed segmentation framework

Herein, we summarize the proposed segmentation framework. The schematic procedure of the proposed framework is shown in Fig.1.

The proposed framework includes the following pre-processing steps: (1) extraction of brain from MR data using the ground truth mask. In practice, it is assumed that all the MR data are skull-stripped, (2) Normalization of intensity values for the multimodal MR brain images to the interval [0 1] using the linear histogram stretching[17], and (3) Co-registration of *a* priori spatial tissue probability maps, obtained from the International Consortium for Brain Mapping (ICBM) [26,27], to the MR brain data by employing the Flirt registration tool in FSL [28]. Given that these preliminary requirements are satisfied, the proposed framework segmenting the MR brain into three tissue types; WM, GM and CSF is as follows.

1. The adaptive bandwidth h_i for each feature point $\mathbf{x}_i$ was estimated by employing the Bayesian-based estimator as described in [22].
2. The modes or clusters $\{\mathbf{z}_1, \mathbf{z}_2, \mathbf{z}_3, \ldots, \mathbf{z}_m\}$ of the MR brain were then computed using the adaptive bandwidth h_i, obtained from the fist step, in Eq.1. The clustering was done in the joint spatial-intensity domain using the joint kernel, defined in Eq.2.
3. Finally, the fuzzy c-means algorithm was applied to categorize the clusters, obtained from the step 2, into the WM, GM, and CSF tissue by employing the Eq.3, wherein the center of the tissues μ was initialized by incorporating the *a* priori spatial tissue probability maps using the Eq.4.

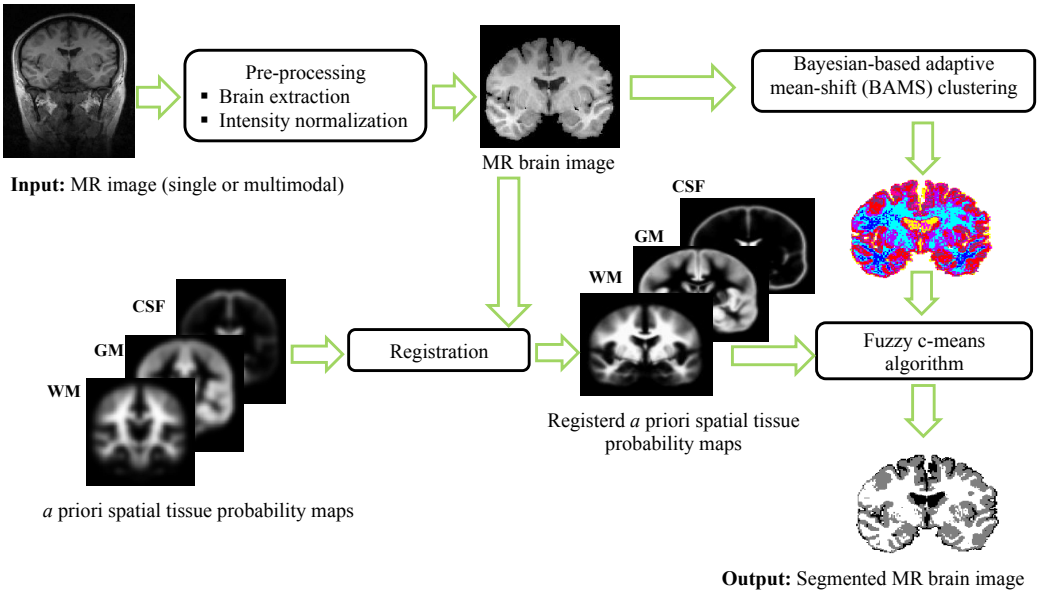

Figure.1 Schematic of the proposed framework for segmenting the WM, GM and CSF tissue in MR images.

2.5. Segmentation performance

The segmentation accuracy of the proposed framework and the other competing methods was evaluated quantitatively, relative to the ground truth in terms of Dice index (DI) [29] and Tanimoto coefficient (TC) [17]. Both metrics are used to measure the degree of overlap between the ground truth and the segmentation result. They are defined as

Downloaded From: http://spiedigitallibrary.org/ on 09/29/2014 Terms of Use: http://spiedl.org/terms

$$DI = \frac{2V_{ae}}{(V_a+V_e)} \tag{7}$$

$$TC = \frac{V_{ae}}{(V_a+V_{e-}V_{ae})} \tag{8}$$

where V_{ae} is the number of voxels the segmentation result and the ground truth have in common, and V_a and V_e denote the number of voxels in the segmentation result and the ground truth respectively. The DI or TC has value one for perfect segmentation and zero when there is no overlap between the segmentation result and ground truth.

3. Experimental results

In this section, we present the experimental results of the proposed framework and the competing methods using the two data sets.

The quantitative results of the proposed framework and our previous method BAMS for the data set 1 for 4 different noise levels with 20% and 40% spatial intensity inhomogeneity level are shown in Fig. 2 and Fig. 3 respectively. They show that the proposed framework has higher Dice index values for each tissue compared to the previous method, based on the mode pruning and voxel weighted k-means.

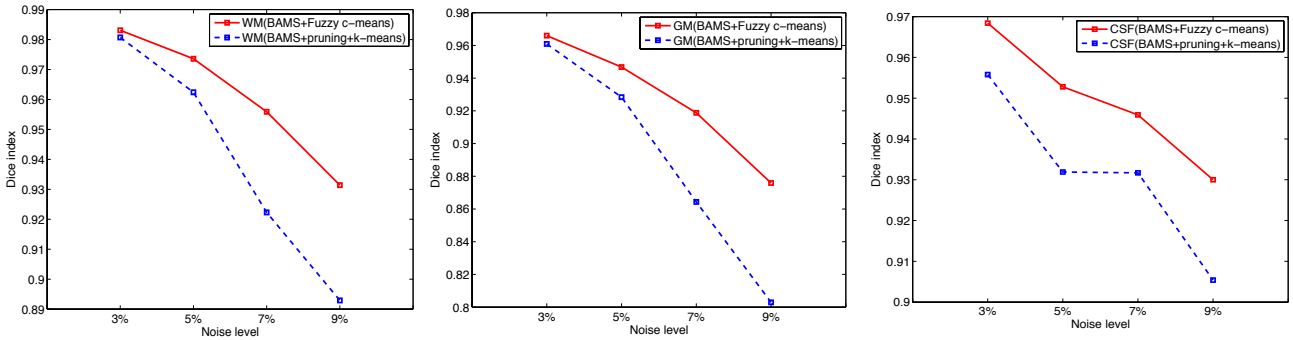

(a) (b) (c)

Figure. 2. The Dice index values for synthetic data for noise levels ranging from 3% to 9% with level of 20% spatial intensity inhomogeneity for (a) WM (b) GM and (c) CSF.

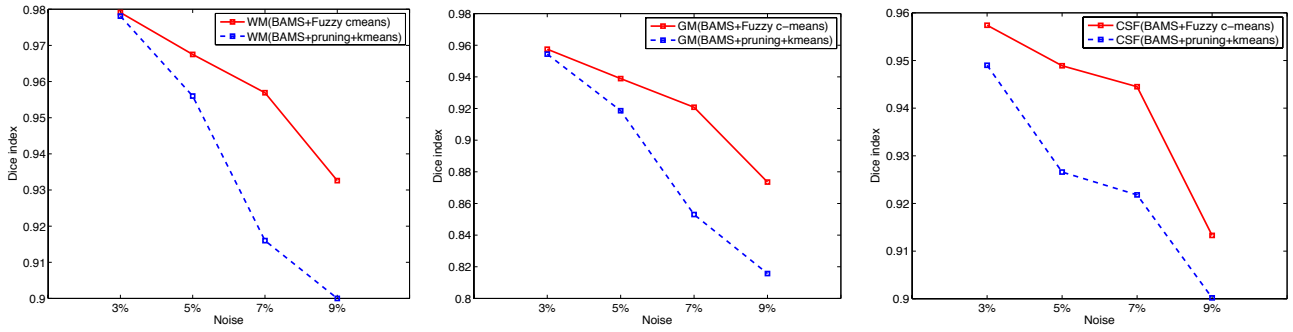

(a) (b) (c)

Figure. 3. The Dice index values for synthetic data for noise levels ranging from 3% to 9% with level of 40% spatial intensity inhomogeneity for (a) WM (b) GM and (c) CSF.

Downloaded From: http://spiedigitallibrary.org/ on 09/29/2014 Terms of Use: http://spiedl.org/terms

An example of the segmentation result of the proposed framework and our previous method for the data set 1 with 9% noise and 40% spatial intensity inhomogeneity level is shown in Fig. 4 (e, f).

The quantitative results for the data set 2 are shown in Fig. 5. They show that the proposed framework has higher segmentation accuracy (higher Tanimoto coefficient) for each tissue compared to the previous method as well as the other competing adaptive mean shift (AMS) framework [17].

An example of the segmentation result of the proposed framework and our previous method for the real T1 weighted image (5_8) from the data set 2 is shown in Fig. 6 (c, d).

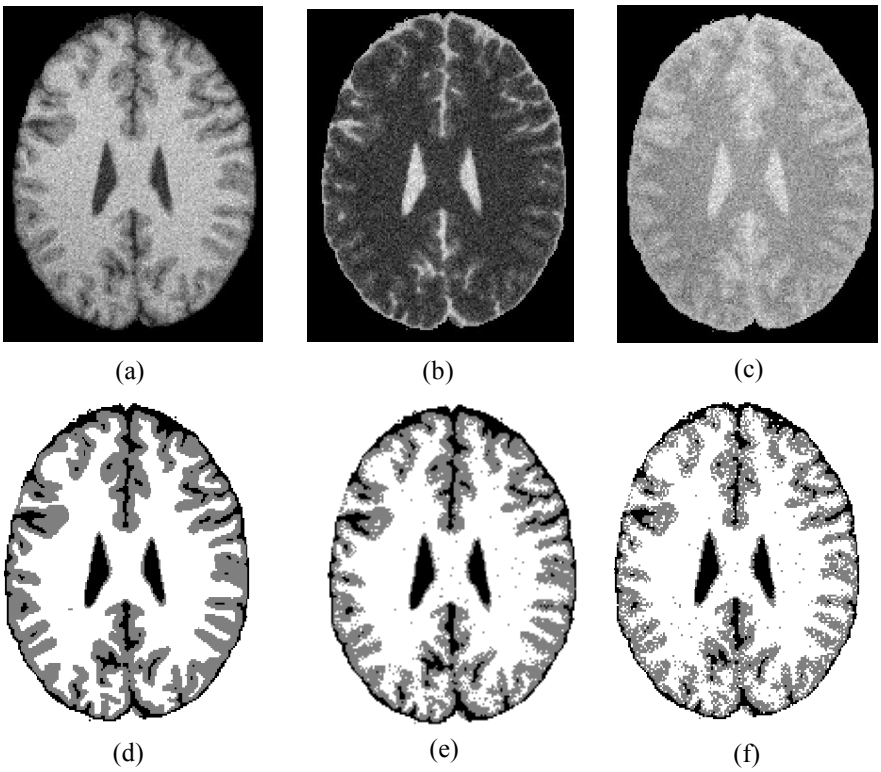

Figure. 4. A sample slice from the BrainWeb: (a-c) Input slice: T1, T2 and PD (proton density) image for 9% noise level with 40 % spatial intensity inhomogeneity (d) Ground truth (e) Proposed framework (f) BAMS + pruning + voxel weighted k-means (WM in white, GM in gray and CSF in black).

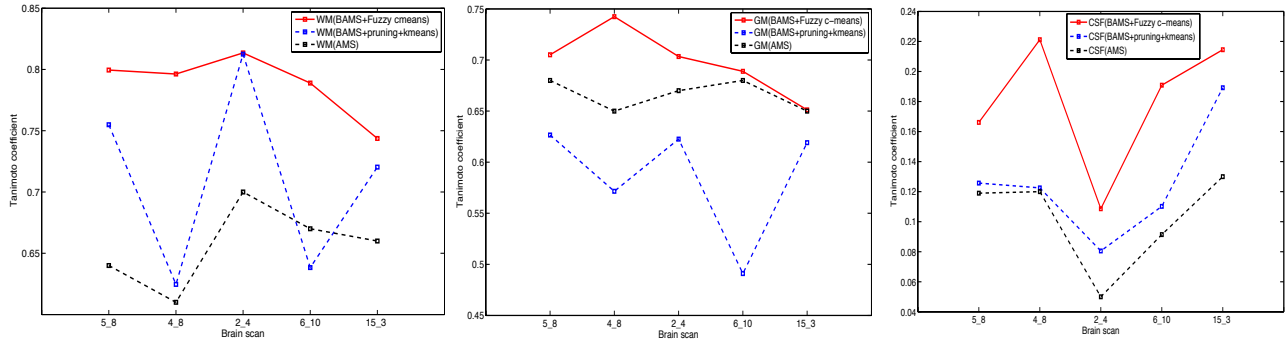

Figure. 5. The Tanimoto coefficient values for real data (five T1-weighted images) for (a) WM (b) GM and (c) CSF.

Downloaded From: http://spiedigitallibrary.org/ on 09/29/2014 Terms of Use: http://spiedl.org/terms

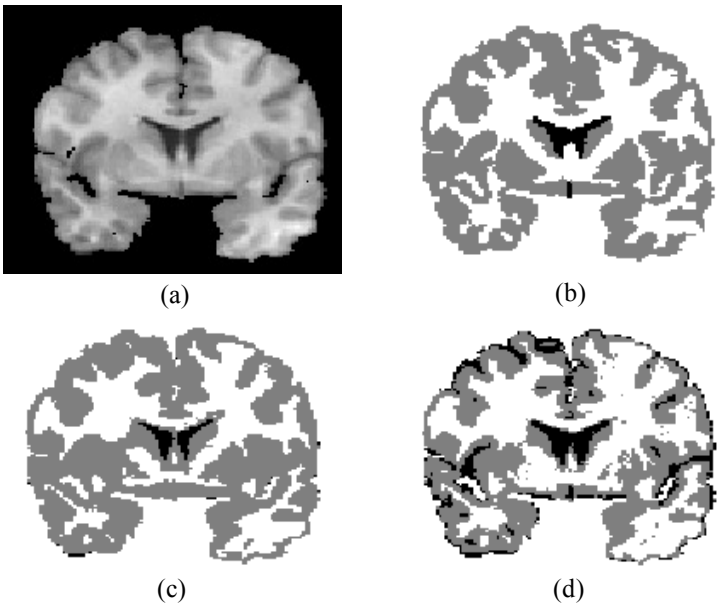

Figure. 6. A sample slice from the IBSR: (a) Input slice: T1 weighted image (5_8) (b) Ground truth (c) Proposed framework (d) BAMS + pruning + voxel weighted k-means (WM in white, GM in gray and CSF in black).

4. Discussion

We presented a new fully automatic unsupervised segmentation framework for the segmentation of three tissue types from the MR brain images. The framework is based on the Bayesian-based adaptive mean shift (BAMS) to initially divide the brain into a number of clusters and on the fuzzy c-means algorithm wherein the *a* priori spatial tissue probability maps are incorporated to categorize the resulting clusters into WM, GM and CSF tissue. We also presented the evaluation of the segmentation accuracy of the proposed framework relative to our previous method as well as to other existing AMS framework [17]. The evaluation was performed using two different data sets: multimodal synthetic MR data from the BrainWeb for the noise levels ranging from 3% to 9% with spatial intensity inhomogeneity levels of 20% and 40% respectively, and five T1-weighted real MR images, corrupted with spatial intensity inhomogeneity, from the IBSR database.

The data set 1 was used to investigate the robustness of the proposed framework relative to our previous method against both noise and spatial intensity inhomogeneity artifacts.

The quantitative results (DI) show that using the *a* priori spatial probability maps in the proposed framework significantly improved the accuracy of segmentation of each tissue for each noise level with each spatial intensity inhomogeneity level compared to the previous method, based on the mode pruning and voxel weighted k-means algorithm.

The qualitative results in Fig. 4 show the robustness of the proposed framework against the noise and spatial intensity inhomogeneity relative to our previous method. It can be observed that the assigning of the clusters to the desired tissue types using the mode pruning and voxel weighted k-means algorithm have a higher tendency to misclassify the WM as GM and the GM as CSF compared to the proposed framework.

The five real T1-weighted images from the data set 2 are acknowledged in literature [17] as difficult to segment because they have varying contrast and strong spatial intensity inhomogeneity across the slices. For this reason, we segmented

Downloaded From: http://spiedigitallibrary.org/ on 09/29/2014 Terms of Use: http://spiedl.org/terms

each T1-weighted image in data set 2 slice by slice using both our proposed framework and previous method. The slice-by-slice segmentation was performed in the coronial direction. The segmented results of the proposed framework and our previous method are also compared with the published results of the existing AMS framework [17], based on the mode pruning and voxel weighted k-means algorithm.

The quantitative results (TC) show that the performance of proposed framework is consistent across the five T1 weighted images with varying contrast and large spatial intensity inhomogeneity compared to competing methods. It outperforms the previous method for each tissue classification except for the case of T1- weighted image (2_4) where it is comparable to previous method for the WM classification. It can also be observed that the slice-by-slice segmentation of data set 2 using the *a* priori spatial tissue probability maps in the proposed framework provides highest segmentation accuracy of each tissue compared to the existing AMS framework, which was applied to segment the whole brain volume with rudimental spatial intensity inhomogeneity correction.

The qualitative results in Fig. 6 show that the mode pruning and the voxel weighted k-means algorithm in the previous method caused the over-segmentation of WM and CSF tissue, which lead to more misclassification of GM compared to the proposed framework. This corroborates the results shown in Fig. 5.

5. Conclusions

We have proposed and evaluated a fully automatic unsupervised framework for segmenting the WM, GM and CSF tissue from the multimodal synthetic and real MR brain images. We demonstrated the robustness of the proposed framework against the noise and spatial intensity inhomogeneity. Integrating the *a* priori spatial tissue probability maps in the fuzzy c-means algorithm to assigning the clusters (modes) to the three desired tissue types improves the segmentation accuracy compared to the competing methods, based on the mode pruning and the voxel weighted k-means algorithm. In addition this increases the segmentation reproducibility of the proposed framework with respect to our previous method.

REFREENCES

1. Courchesne, E., Chisum, H. J., Townsend, J., Cowles, A., Covington, J., Egaas, B., Harwood, M., Hinds, S., and Press, G. A., "Normal Brain Development and Aging: Quantitative Analysis at in Vivo MR Imaging in Healthy Volunteers," Radiology, 216(3), 672-682 (2000).
2. Simmons, A., Westman, E, Muehlboeck, S., Mecocci, P., Vellas, B., Tsolaki, M., Kloszewska, I., Wahlund, L., Soininen, H., Lovestone, S., Evans, A., and Spenger, C., "MRI measures of Alzheimer's disease and the AddNeuroMed study," Ann N Y Acad Sci., 1180, 47-55 (2009) .
3. Daryoush, M., Kouzani, A. Z., and Soltanian-Zadeh, H., "Segmentation of multiple sclerosis lesions in MR images: a review," Neuroradiology, 54, 299–32 (2012).
4. Rullmann, M., Anwander, A., Dannhauer, M., Warfield, S. K., Duffy, F.H., and Wolters, C. H., "EEG source analysis of epileptiform activity using a 1 mm anisotropic hexahedra finite element head model," NeuroImage, 44(2), 399–410 (2009).
5. Shirvany, Y., Mahmood, Q., Edelvik, F., Persson, M., Hedstrom, A., and Jakobsson, S., "Particle Swarm Optimization Applied to EEG Source Localization of Somatosensory Evoked Potentials," IEEE Trans Neural Syst. Rehabil. Eng., 22(1), 11-20 (2013).
6. Fortunati, V., Verhaart, R. F., van der Lijn, F., Niessen, W. J., Veenland, J. F., Paulides, M. M., and Walsum, T., van, "Hyperthermia critical tissues automatic segmentation of head and neck CT images using atlas registration and graph cuts," Proc. ISBI, 1683-1686 (2012) .
7. Fortunati, V., Verhaart, R. F., van der Lijn, F., Niessen, W. J., Veenland, J. F., Paulides, M. M., and Walsum, T., van, "Tissue segmentation of head and neck CT images for treatment planning: A multiatlas approach combined with intensity modeling," Medical Physics, 40, 071905 (2013).
8. Liu, H., Yang, C., Pan, N., Song, E., and Green, R., "Denoising 3D MR images by the enhanced non-local means filter for Rician noise," Magnetic Resonance Imaging, 28(10), 1485–1496 (2010).

Downloaded From: http://spiedigitallibrary.org/ on 09/29/2014 Terms of Use: http://spiedl.org/terms

9. Hu, J., Pu, Y., Wu, X., Zhang, Y., and Zhou, J., "Improved DCT-Based Nonlocal Means Filter for MR Images Denoising," Computational and Mathematical Methods in Medicine, Article ID 232685, 14 pages (2012).
10. Simmons, A., Tofts, P. S., Barker, G. J., and Arridge, S. R., "Sources of intensity nonuniformity in spin echo images at 1.5 T," Magn Reson Med., 32(1), 121-8 (1994).
11. Li, X., Li, L., Lu, H., and Liang, Z., "Partial Volume Segmentation of Brain Magnetic Resonance Images Based on Maximum a Posteriori Probability," Med Phys., 32(7), 2337–2345 (2005).
12. Wells, W. M., Grimson, W. E. L., Kikinis, R., and Jolesz, F. A.,"Adaptive segmentation of MRI data," IEEE Trans. Med. Imag., 13, 429–442 (1996).
13. Held, K., Kops, E. R., Krause, B. J., Wells, W. M., Kikinis, R., and Müller-Gärtner, H.W., "Markov random field segmentation of brain MR images," IEEE Trans. Med. Imag., 16, 878–886 (1997).
14. Kapur, T., Grimson, W. E. L., Kikinis, R., and Wells, W. M., "Enhanced spatial priors for segmentation of magnetic resonance imaging," Proc. MICCAI, 1496, 457–468 (1998).
15. Leemput, K. Van, Maes, F., Vandermeulen, D., and Suetens, P., "Automated model-based tissue classification of MR images of the brain," IEEE Trans. Med. Imag., 18(10), 897-908 (1999).
16. Marroquín, J. L., Vemuri, B. C., Botello, S., and Calderon, F., "An accurate and efficient Bayesian method for automatic segmentation of brain MRI, " IEEE Trans. Med. Imag., 21(8), 934–944 (2002).
17. Mayer, A., and Greenspan, H., "An adaptive mean-shift framework for MRI brain segmentation," IEEE Trans. Med. Imag., 28(8), 1238–1249 (2009).
18. Fukunaga, K., and Hostetler, L., "The estimation of the gradient of a density function, with applications in pattern recognition," IEEE Transactions on Information Theory, 21(1), 32-40 (1975).
19. Comaniciu, D., and Meer, P., "Mean shift: a robust approach toward feature space analysis," IEEE Transactions on Pattern Analysis and Machine Intelligence, 24(5), 603-619 (2002).
20. Comaniciu, D., "An algorithm for data-driven bandwidth selection," IEEE Trans. Pattern Anal. Mach. Intell., 25(2), 281–288 (2003).
21. Georgescu, B., Shimshoni, I., and Meer, P., "Mean-shift based clustering in high dimensions: A texture classification example," Proc. ICCV, 456–463 (2003).
22. Mahmood, Q., Chodorowski, A., Mehnert, A., and Persson, M., "A Novel Bayesian Approach to Adaptive Mean Shift Segmentation of Brain Images," Proc. CBMS (Computer-Based Medical Systems), 1-6 (2012).
23. BrainWeb, http://brainweb.bic.mni.mcgill.ca/brainweb/.
24. Internet Brain Segmentation Repository Center for Morphometric Analysis (IBSR), http://www.cma.mgh.harvard.edu/ibsr.
25. Bezdek, J. C., Pattern Recognition with Fuzzy Objective Function Algorithms, Kluwer Academic Publishers, Norwell, MA, USA (1981).
26. International Consortium for Brain Mapping (ICBM), http://www.loni.ucla.edu/ICBM/Downloads/Downloads_ICBMprobabilistic.shtml.
27. Statistical Parametric Mapping (SPM), http://www.fil.ion.ucl.ac.uk/spm/.
28. Jenkinson, M., Bannister, P.R., Brady, J.M., and Smith, S.M., "Improved optimisation for the robust and accurate linear registration and motion correction of brain images," NeuroImage, 17(2), 825-841 (2002).
29. Dice, L. R., "Measures of the amount of ecologic association between species," Ecology, 26, 297–302 (1945).

Downloaded From: http://spiedigitallibrary.org/ on 09/29/2014 Terms of Use: http://spiedl.org/terms